THE INFLUENCE OF MAIN DESIGN PARAMETERS ON HELICOPTER AIR RESONANCE AND ITS SOURCE OF INSTABILITY

Zhang, Xiaogu
Professor
Nanjing Aeronautical Institute
Nanjing, P. R. China

Abstract

Helicopter air resonance, a serious airborne rotor/body coupled dynamic instability problem, is studied with complex multiblade coordinates. The source of instability is the mutual excitation between two degree-of-freedom. A method to analyze the excitation (work done by one degree-of-freedom on another degree-of-freedom) is developed. The source of instability, the influence of main design parameters and their physical explanation are investigated through the analysis of mutual excitation, eigenvalue and eigenvector (mode shape). One source of instability is the mutual excitation between regressive lead-lag motion and body forward whirling motion stemming from their inertial coupling. Another source is the mutual excitation between lead-lag motion and flap motion which is proportional to rotor lift. The rotor with low flap frequency and high lead-lag frequency is more vulnerable to air resonance instability. The influence of other parameters is also discussed.

Notation

a = blade airfoil lift-curve slope, $rad^{-1}(2\pi)$
b = blade chord
c_x = blade airfoil profile drag coeffient
E = work done by one degree of freedom on another degree of freedom
h = distance from body C. G. to rotor plane
I = imaginary part of the eigenvector
$I_b = \int_0^1 \frac{dM_b}{d\bar{r}}\bar{r}^2 d\bar{r}$, blade flap or lead-lag inertia
I_{fx}, I_{fy} = body roll and pitch inertia about body C. G
$\bar{I}_x, \bar{I}_y = \frac{(I_{fx}+h^2NM_b)}{\frac{N}{2}I_bR^2}, \frac{(I_{fy}+h^2NM_b)}{\frac{N}{2}I_bR^2}$
$\bar{I}_h, \delta\bar{I}_h = (\frac{\bar{I}_x+\bar{I}_y}{2}), (\frac{\bar{I}_x-\bar{I}_y}{2})$
M_b = mass of one blade
N = number of blades
r = blade radial staion
R = blade radius
= real part of the eigenvector
β_k = perturbation flapping motion of the kth blade
β_0 = equilibrium flapping angle (coning angle), rad
$\gamma = \frac{\rho a \bar{b} R^3}{I_b}$, blade Lock number
θ = blade collective pitch angle, rad
$\lambda = \sigma + i\omega$, eigenvalue
ξ_k = perturbation lead-lag motion of the kth blade
ξ_0 = equilibrium lag angle, rad
ρ = air density
σ = real part of eigenvalue
$= \frac{Nb}{\pi R}$, rotor solidity
φ_0 = initial value of body motion φ
φ_x, φ_y = body roll and pitch motion, rad
ψ_k = azimuth angle of the kth blade, rad
Ω = rotor angular velocity
Ω_0 = rotor normal speed
ω = imaginary part of eigenvalue
ω_β, ω_ξ = uncoupled fundamental flap and lead-lag frequencies
$\dot{(\ )}$ = $d(\ )/d\psi$
$\bar{(\ )}$ = $(\ )/R$, made dimensionless by rotor radius
= $(\ )/\Omega$, made dimensionless by rotor speed
= conjugate of complex variable
$(\ )_a$ = refer to forward whirling component
$(\ )_b$ = refer to backward whirling component

Introduction

Helicopter air resonance is an airborne rotor/body coupled instability problem. It is caused by the coupling of rotor regressive lead-lag motion and rigid fuselage pitch and roll rotation. There is also considerable participation of blade flap motion and rotor aerodynamics. Air resonance can happen only in soft-inplane rotors (the blade fundamental lead-lag natural frequency ω_ξ is less than rotor rotational speed Ω). Typically, the frequency of the unstable mode is approximately equal to ω_ξ in the rotating coordinate and $\Omega - \omega_\xi$ in the nonrotating coordinate.

Previous works investigated the nature of this phenomenon and provided a basis for the practical solution[1,2,3]. Nevertheless, the understanding of its source of instability and the influence of main design parameters is still inadequate. The purpose of this work is to obtain a clear understanding in these aspects.

Air resonance is the self-excited vibration of a dynamic system with multi-degrees of freedom. The source of in stability is the positive mutual excitation between two or more degrees of freedom (to do positive work mutually). Clear description of the mode shape (eigenvector) is necessary to the investigation of mutual exci-

tation. Complex coordinates, which are superior to the conventional longitudinal and lateral coordinates in the analysis of mode shape, are adopted in this work. The complex coordinates were first adopted by coleman in the analysis of helicopter ground resonance[4]. But his work is limited to the analysis of eigenvalues. Since the complex variable is not superior in this aspect, it has not been widely adopted. In Ref. 5, the complex coordinates were adopted again to analyze not only the eigenvalues, but also the eigenvectors in the analysis of air resonance in vacuo, and were proved to be valuable for the clear description of mode shapes.

Based on the complex coordinates adopted, a method to analyze the mutual excitation quantitatively is developed in this work. Approximate simple expressions of the mutual excitations are derived which can be used to explain the influence of main design parameters. This idea was first suggested by Bielawa as the "Force-Phasing Matrix" method[6]. Since the longitudinal and lateral coordinates were still used in his analysis, his investigation on air resonance was unsuccessful.

This work is limited to the hover condition.

Analytical Model

The model shown in Fig. 1 is as simple as possible but still retains the fundamental characters of helicopter air resonance. The main assumptions are:

1) Only rigid fuselage pitch and roll rotation about body center of gravity (φ_y, φ_x) are taken into account.

2) Only the fundamental blade flap and lead-lag mode are taken into account, the mode shape is simplified as a straight line.

3) There is no structural coupling between flap and leag-lag motion, the blade pitch d. o. f. (deree of freedom) is not retained.

4) The blade mass is distributed uniformlly along the span and the planform is rectangular. There is no geometrical twist.

5) Linear aerodynamics, quasisteady assumption. The dynamic inflow is not taken into account.

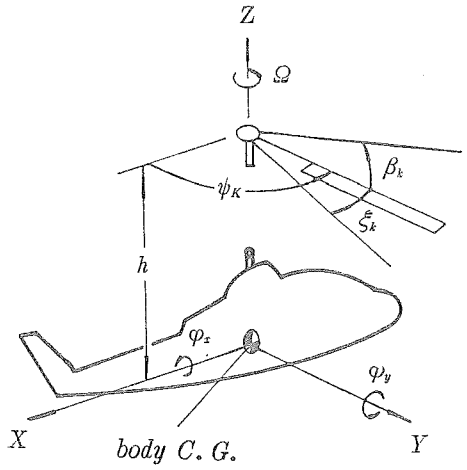

Fig. 1 Analytical model of helicopter air resonance

The individual blade flap and lead-lag motions (β_k, ξ_k) are combined together and transfered to the nonrotating coordinate through multiblade transformation as below

$$\beta_c = \frac{2}{N}\sum_{k=1}^{N}\beta_k\cos(\psi_k - \xi_0), \beta_s = \frac{2}{N}\sum_{k=1}^{N}\beta_k\sin(\psi_k - \xi_0)$$
$$\xi_c = \frac{2}{N}\sum_{k=1}^{N}\xi_k\cos(\psi_k - \xi_0), \xi_s = \frac{2}{N}\sum_{k=1}^{N}\xi_k\sin(\psi_k - \xi_0) \quad (1)$$

β_c, β_s are equivalent to the longitudinal and lateral rotor disc-plane tilt. ξ_c, ξ_s represent the lateral and longitudinal rotor lead-lag motion. Only these four variables can be coupled with the hub center motion induced from the body rotation. Hence, the rotor/body coupled system consists of a total of six degrees of freedom.

In this work the flap, lead-lag and body freedoms are each combined into one complex variable.

$$\beta = \beta_c + i\beta_s, \xi = \xi_c + i\xi_s, \varphi = \varphi_x + i\varphi_y \quad (2)$$

The equations of motion are derived by Newtonian method. The nonlinear equations are linearized about the steady equilibrium condition. The equations are of the form

$$[M]\{\ddot{x}\} + [C]\{\dot{x}\} + [K]\{x\} = 0 \quad (3)$$

M, C and K are the mass, damping, and stiffness matrices respectively. the matrix elements are given in the Appendix.

For the isotropic case (inertial isotropy of the fuselage, $I_{fx} = I_{fy}$), the degrees of freedom are

$$\{x\} = \{\beta, \xi, \varphi\}^T \quad (4)$$

The resulatant motion is a kind of one-directional whirling motion. The expressions are

$$\beta = \beta_0 e^{\lambda\psi}, \xi = \xi_0 e^{\lambda\psi}, \varphi = \varphi_0 e^{\lambda\psi} \quad (5)$$

$\psi = \Omega t$ is used instead of the time variable t. Hence, the eigenvalue $\lambda = \sigma + i\omega$ is nondimensionalized to rotor speed Ω.

The imaginary part of the eigenvalue ω represents not only the modal frequency but also the direction and angular velocity of the whirling motion. If ω is positive, the whirling is forward, otherwise backward. Here 'forward' and 'backward' refer to the direction of rotor rotaion. The rotor motion can be tranfered from nonrotating coordinate to rotating coordinate by multiplying $e^{-i\psi}$. If the resultant algebraic sum of the imaginary part is negative, the rotor motion is a regressive mode, if positive then it is an advancing mode.

The real part of the eigenvalue σ represents the modal damping. If σ is positive, the motion is divergent (negative damping), otherwise convergent (positive damping). Besides, it also represents the direction and veloocity in the radial sense.

the eigenvectors are normalized to body motion φ:

$$\beta/\varphi = R_1 + iI_1, \xi/\varphi = R_2 + iI_2 \quad (6)$$

Besides, $\xi/\beta = R_{12} + iI_{12}$ is also used to express the relationship between ξ and β.

The eigenvectors have difinite geometrical meaning and represent the relationship between two different d. o. f. For example, R_2 and I_2 represent the relationship between lead-lag motion and body or hub center motion

(Fig. 2). R_2 represents the radial lead-lag motion and I_2 represents the tangential lead-lag motion. Similarly R_1 represents tangential disc-plane tilt and I_1 represents radial disc-plane tilt.

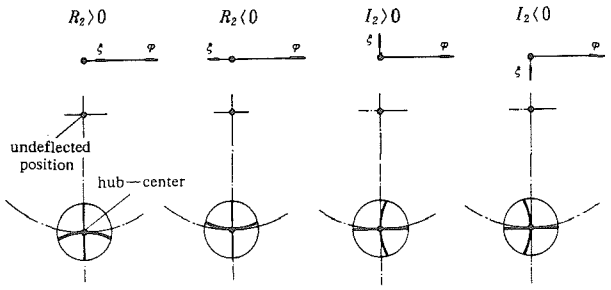

Fig. 2 The relationship between blade lead-lag motion and hub center motion due to eigenvector ξ/φ

The eigenvalue and eigenvector combined together fully describe the resultant motion.

For the nonisotropic case ($I_{fx} \neq I_{fy}$) the resultant motion is a combination of two counter-whirling motions

$$\begin{aligned} \beta &= \beta_a + \beta_b = \beta_{ao}e^{\lambda\psi} + \beta_{bo}e^{\bar{\lambda}\psi} \\ \xi &= \xi_a + \xi_b = \xi_{ao}e^{\lambda\psi} + \xi_{bo}e^{\bar{\lambda}\psi} \\ \varphi &= \varphi_a + \varphi_b = \varphi_{ao}e^{\lambda\psi} + \varphi_{bo}e^{\bar{\lambda}\psi} \end{aligned} \tag{7}$$

$\bar{\lambda}$ is the conjugate of λ . The subscript "a" denotes the forward whirling motion and "b" denotes the backward whirling motion. The degrees of freedom in this case are

$$\{x\} = \{\beta_a, \bar{\beta}_b, \xi_a, \bar{\xi}_b, \varphi_a, \bar{\varphi}_b\}^T \tag{8}$$

$\bar{\beta}_b, \bar{\xi}_b$, and $\bar{\varphi}_b$ are conjugates of β_b, ξ_b and φ_b .

The eigenvectors are

$$\begin{aligned} \beta_a/\varphi_a &= R_{1a} + iI_{1a} \\ \beta_b/\varphi_b &= R_{1b} + iI_{1b} \\ \xi_a/\varphi_a &= R_{2a} + iI_{2a} \\ \xi_b/\varphi_b &= R_{2b} + iI_{2b} \\ \bar{\varphi}_b/\varphi_a &= R_3 + iI_3 \end{aligned} \tag{9}$$

Besides, $\xi_a/\beta_a = R_{12a} + iI_{12a}$ and $\xi_b/\beta_b = R_{12b} + iI_{12b}$ are also used to express the relationship between ξ_a and β_a , ξ_b and β_b .

The combination of two counter-whirling motions forms a kind of elliptical whirling motion. The whirling direction and the position of the major axis can be derived from the eigenvector.

It is interesting to note the form of the matrix elements of the nonisotropic case. The M matrix of the nonistropic case is formed by the M matrix elements and their conjugates of the isotropic case and coupling term $\delta\bar{I}_h$.

$$[M] = \begin{bmatrix} M_{11} & M_{12} & M_{13} \\ M_{21} & M_{22} & M_{23} \\ M_{31} & M_{32} & M_{33} \end{bmatrix} \cdots\cdots isotropic$$

$$[M] = \begin{bmatrix} M_{11} & 0 & M_{12} & 0 & M_{13} & 0 \\ 0 & \bar{M}_{11} & 0 & \bar{M}_{12} & 0 & \bar{M}_{13} \\ M_{21} & 0 & M_{22} & 0 & M_{23} & 0 \\ 0 & \bar{M}_{21} & 0 & \bar{M}_{22} & 0 & \bar{M}_{23} \\ M_{31} & 0 & M_{32} & 0 & M_{33} & \delta\bar{I}_h \\ 0 & \bar{M}_{31} & 0 & \bar{M}_{32} & \delta\bar{I}_h & \bar{M}_{33} \end{bmatrix} \cdots\cdots nonisotropic \tag{10}$$

The C and K matrices of the nonisotropic case are formed by the matrix elements and their conjugates of the isotropic case in the same procedure, except that there are no such coupling terms as $\delta\bar{I}_h$ in the $[M]$ matrix.

In view of these expressions of the nonisotropic case, it is apparent that there are no opposite whirling components in the equilibrium equations, such as β_b, ξ_b and φ_b in the equibrium equations of β_a and ξ_a , except φ_b in the equation of φ_a and vice versa. Hence the complex variables $\beta_a, \xi_a, \varphi_a$ are orthogonal to β_b, β_b and $\beta_b, \xi_b, \varphi_b$ are orthogonal to β_a, ξ_a . If the longitudinal and lateral coordinates are adopted, the lateral variables β_s, ξ_c and φ_x will appear in the longitudinal equilibrium equations and vice versa. That is the main difference between these two kinds of variables.

Mutual Excitation

The excitation of the isotropic case E_{pq} is the work done by qth d. o. f. (degree of freedom) on the pth d. o. f. which can be expressed as the dot product of the generalized forces acting on the pth d. o. f. by the qth d. o. f. and the "velocity" of the pth d. o. f.. E_{pq} can be derived from the equilibrum equation of the pth d. o. f. through the following relationship

$$\begin{aligned} E_{12} &= -[M_{12}, C_{12}, K_{12}]\{\ddot{\xi}, \dot{\xi}, \xi\}^T \cdot (\dot{\beta} - i\beta) \\ E_{13} &= -[M_{13}, C_{13}, K_{13}]\{\ddot{\varphi}, \dot{\varphi}, \varphi\}^T \cdot (\dot{\beta} - i\beta) \\ E_{21} &= -[M_{21}, C_{21}, K_{21}]\{\ddot{\beta}, \dot{\beta}, \beta\}^T \cdot (\dot{\xi} - i\xi) \\ E_{23} &= -[M_{23}, C_{23}, K_{23}]\{\ddot{\varphi}, \dot{\varphi}, \varphi\}^T \cdot (\dot{\xi} - i\xi) \\ E_{31} &= -[M_{31}, C_{31}, K_{31}]\{\ddot{\beta}, \dot{\beta}, \beta\}^T \cdot \dot{\varphi} \\ E_{32} &= -[M_{32}, C_{32}, K_{32}]\{\ddot{\xi}, \dot{\xi}, \xi\}^T \cdot \dot{\varphi} \end{aligned} \tag{11}$$

Where subscript "1" denotes the 1st d. o. f. β , "2" denotes the 2nd f. o. f. ξ and "3" denotes the 3rd d. o. f. φ, M_{pq}, C_{pq} and K_{pq} are the appropriate matrix elements.

The final expressions of E_{pq} are functions of eigenvalue, eigenvectors, and elements of matrices.

For the nonisotropic case, E_{pqa} is the work done by the forward whirling components of the qth d. o. f. on the forward whirling components of the pth d. o. f. ; E_{pqb} is the excitation of the backward whirling components of the qth d. o. f. on the backward whirling components of the pth d. o. f.

$$\begin{aligned} E_{12a} &= -[M_{12}, C_{12}, K_{12}]\{\ddot{\xi}_a, \dot{\xi}_a, \xi_a\}^T \cdot (\dot{\beta}_a - i\beta_a) \\ E_{12b} &= -[M_{12}, C_{12}, K_{12}]\{\ddot{\xi}_b, \dot{\xi}_b, \xi_b\}^T \cdot (\dot{\beta}_b - i\beta_b) \\ E_{13a} &= -[M_{13}, C_{13}, K_{13}]\{\ddot{\varphi}_a, \dot{\varphi}_a, \varphi_a\}^T \cdot (\dot{\beta}_a - i\beta_a) \\ E_{13b} &= -[M_{13}, C_{13}, K_{13}]\{\ddot{\varphi}_b, \dot{\varphi}_b, \varphi_b\}^T \cdot (\dot{\beta}_b - i\beta_b) \\ E_{21a} &= -[M_{21}, C_{21}, K_{21}]\{\ddot{\beta}_a, \dot{\beta}_a, \beta_a\}^T \cdot (\dot{\xi}_a - i\xi_a) \\ E_{21b} &= -[M_{21}, C_{21}, K_{21}]\{\ddot{\beta}_b, \dot{\beta}_b, \beta_b\}^T \cdot (\dot{\xi}_b - i\xi_b) \\ E_{23a} &= -[M_{23}, C_{23}, K_{23}]\{\ddot{\varphi}_a, \dot{\varphi}_a, \varphi_a\}^T \cdot (\dot{\xi}_a - i\xi_a) \\ E_{23b} &= -[M_{23}, C_{23}, K_{23}]\{\ddot{\varphi}_b, \dot{\varphi}_b, \varphi_b\}^T \cdot (\dot{\xi}_b - i\xi_b) \\ E_{31a} &= -[M_{31}, C_{31}, K_{31}]\{\ddot{\beta}_a, \dot{\beta}_a, \beta_a\}^T \cdot \dot{\varphi}_a \end{aligned}$$

$$E_{31b} = -[M_{31}, C_{31}, K_{31}]\{\ddot{\beta}_b, \dot{\beta}_b, \beta_b\}^T \cdot \dot{\varphi}_b$$

$$E_{32a} = -[M_{32}, C_{32}, K_{32}]\{\ddot{\xi}_a, \dot{\xi}_a, \xi_a\}^T \cdot \dot{\varphi}_a$$

$$E_{32b} = -[M_{32}, C_{32}, K_{32}]\{\ddot{\xi}_b, \dot{\xi}_b, \xi_b\}^T \cdot \dot{\varphi}_b \qquad (12)$$

From the previous analysis it is evident that there is no mutual excitation between β_a, ξ_a and $\beta_b, \xi_b, \varphi_b$, between β_b, ξ_b and φ_a.

Analysis of the Results

The most influential design parameters are the ratio of uncoupled blade flap and lead-lag natural frequency to rotor speed Ω ($\bar{\omega}_\beta, \bar{\omega}_\xi$). $\bar{\omega}_\beta$ and $\bar{\omega}_\xi$ range from 1.03, 0.25 (articulated rotor with hinge effset) to 1.15, 0.7 (hingeless rotor) respectively at normal rotor speed Ω_0 for current helicopters. Besides, $\bar{\omega}_\beta$ and $\bar{\omega}_\xi$ vary significantly with Ω for hingeless rotor or articulated rotor with elastical hinge restraint (see Fig. 19). In this work, eigenvalue, eigenvector and mutual excitation versus $\bar{\omega}_\beta$ from 0 to 2 at different $\bar{\omega}_\xi$ are caeculated.

The other parameters used in this analysis are typical for conventional helicopters. The ratio of rotor height to rotor radius $\bar{h} = 0.312$. The rotor solidity $\sigma = 0.08218$. The rotor blade profile drag coefficient $c_x = 0.01$. The Lock number $\gamma = 10$. The ratio of the average value of helicopter roll and pitch inertia (I_x, I_y) to rotor roll or pitch inertia $\bar{I}_h = 6.147$. $\delta\bar{I}_h$ represents the nonidentity of helicopter pitch and roll inertia. For the isotropic case, $\delta\bar{I}_h = 0$. For the nonisotropic case, $\delta\bar{I}_h = -0.5\bar{I}_h (I_y = 3I_x)$.

Rotor lift and coning angle β_0 are nearly proportional to blade collective pitch angle θ. As mentioned in previous works[7,8], θ is influential to air resonance instability. θ ranges from zero to 0.3 rad in this investigation.

The variation of eigenvalues versus rotor speed for typical rotor types is also calculated to investigate the instability and unstable speed range of actual helicopters.

The Case with Zero Collective Pitch ($\theta = 0$)

The variation of eigenvalues with $\bar{\omega}_\beta$ for the isotropic case is shown in Fig. 3., $\bar{\omega}_\xi = 0.8$ in this case. There are six modes: flap advancing mode (FA), flap regressive mode (FR), lead-lag advancing mode (LA), lead-lag regressive mode (LR), gyroscopic mode (GS), and a zero root mode. The FA, LA and LR modes are forward whirling modes (positive ω). ω of the FA and LA modes is close to $1+\bar{\omega}_\beta$ and $1+\bar{\omega}_\xi$ respectively. In the rotating coordinate, they are advancing modes and their frequency is close to $\bar{\omega}_\beta$ and $\bar{\omega}_\xi$ respectively. ω of the LR mode is nearly equal to $1-\bar{\omega}_\xi$. In the rotating coordinate, its frequency is nearly equal to $-\bar{\omega}_\xi$ and hence it is a regressive mode. The FR and GS modes are regressive modes in the rotating coordinate ($\omega - 1 < 0$). They are partly forward and partly backward in the nonrotating coordinate.

In the case of $\bar{\omega}_\beta = 1.0$ (centrally hinged rotor), σ of the FA and FR modes is -0.625, which is equal to the damping of the uncoupled flap motion $\gamma/16$, and the modal damping of LA and LR modes is close to the uncoupled lead-lag damping $\gamma c_x/4$. The LR mode is the most unstable. The instability of the LR mode increases with the increase of $\bar{\omega}_\beta$ and the decrease of $\bar{\omega}_\xi$ as shown in Fig. 4. Helicopter air resonance is the unstable motion of the LR mode.

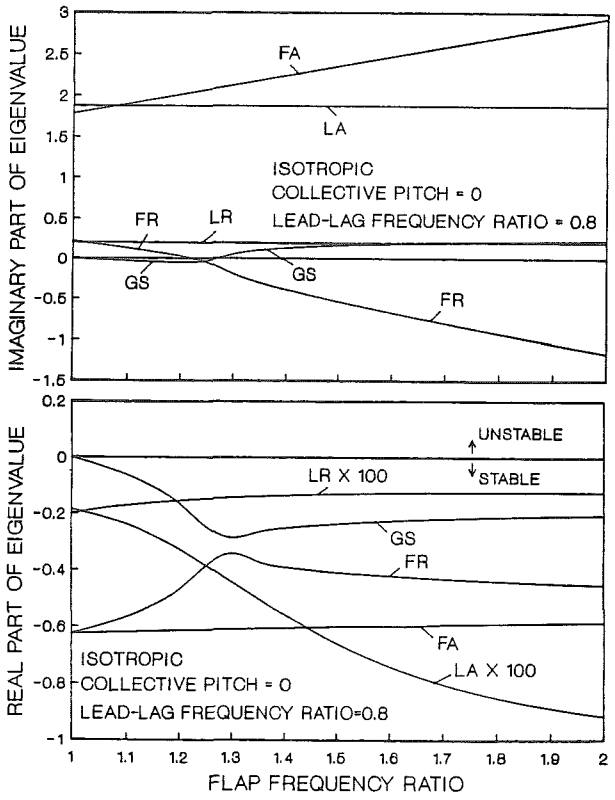

Fig. 3 Eigenvalue versus flap frequency ratio $\bar{\omega}_\beta$ (isotropic, $\bar{\omega}_\xi = 0.8, \theta = 0$)

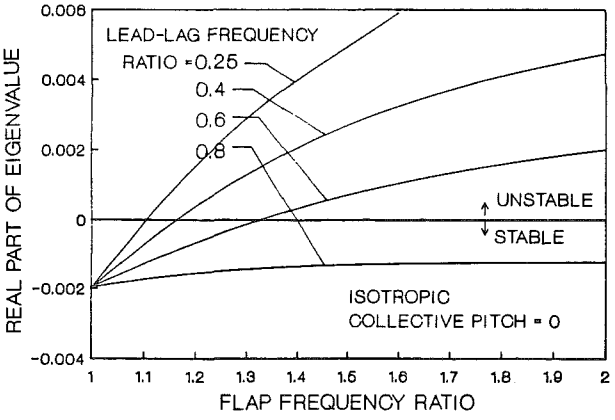

Fig. 4 Real part of eigenvalue of the LR mode (isotropic, $\theta = 0$)

Eigenvector of the LR mode is shown in Fig. 5. $|R_2 + iI_2|$ is much larger than $|R_1 + iI_1|$ and unity. Hence the lead-lag motion is predominant in this mode. R_1 and ω are simultaneously positive which means that the tangential disc-plane tilt is always opposite to the body whirling motion. This can be explained by the character-

istics of the flap response to the body rotation (rotor angular velocity damping).

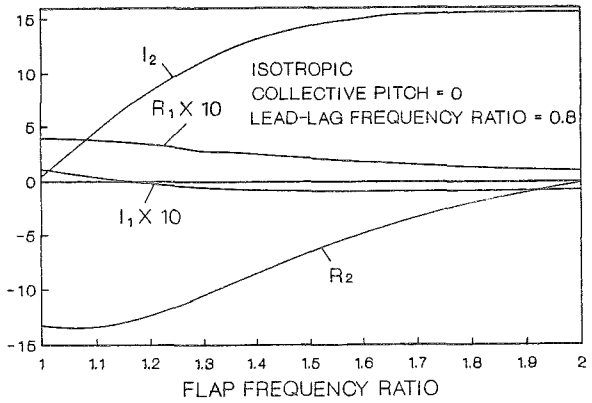

Fig. 5 Eigenvector of the LR mode versus flap frequency $\bar{\omega}_\beta$ (isotropic, $\bar{\omega}_\xi = 0.8, \theta = 0$)

Mutual excitation (normalized to $|\varphi|^2$) of the LR mode is shown in Fig. 6. It is also shown as a diagram in Fig. 7. The arrow denotes the direction of excitation. The sign in the circle denotes positive or negative work.

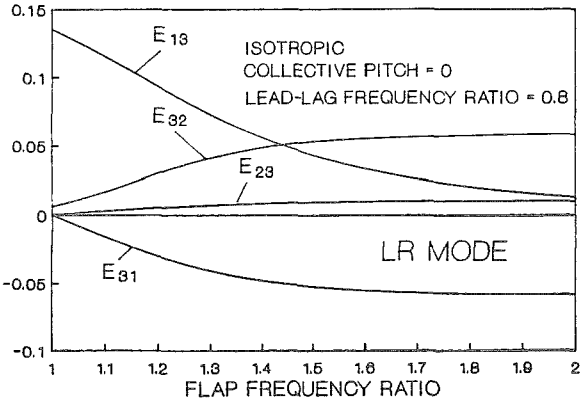

Fig. 6 Mutual excitation of the LR mode (isotropic, $\bar{\omega}_\xi = 0.8, \theta = 0$)

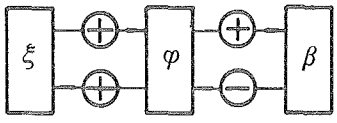

Fig. 7 Diagram of mutual excitation of the LR mode (isotopic, $\theta = 0$)

It is evident that the source of instability is the positive mutual excitation between lead-lag motion and body motion. Furthermore, the expressions of normalized E_{23} and E_{32} can be simplified as

$$E_{23} \approx -\frac{3}{2}\bar{h}\omega^2(\omega - 1)I_2$$
$$E_{32} \approx \frac{3}{2}\bar{h}\omega^3 I_2 \qquad (13)$$

In this case the eigenvector I_2 is positive and the geometrical relationship between the lead-lag motion and hub center motion of this forward whirling mode due to the positive I_2 is shown in Fig. 8. The rotor lead-lag force excites the body in the direction of hub center motion. The inertial force on the blade due to hub center motion is in phase with the blade lead-lag velocity, but the blade motion should be examined in the rotating coordinate. The source of instability is this inertial coupling between the rotor regressive lead-lag motion and the body forward whirling motion.

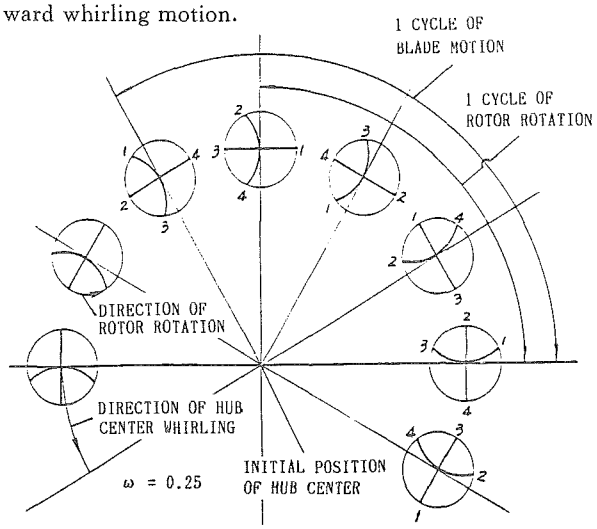

Fig. 8 Illustration of hub center motion and blade lead-lag motion in air resonance

Since the frequency of the LR mode $\omega \approx 1 - \bar{\omega}_\xi$, from equation (13) it is evident that only for the soft-inplane rotor ($\bar{\omega}_\xi < 1$) can E_{23} and E_{32} of the LR mode be simultaneously positive and this mode be unstable. The increase of instability with the decrease of $\bar{\omega}_\xi$ shown in Fig. 4 can be explained by the increase of E_{23} and E_{32} due to the increase of ω. The increase of instability with $\bar{\omega}_\beta$ shown in Fig. 4 can be explained by the increase of E_{23} and E_{32} due to the increase of I_2 (Fig. 5).

E_{31} is negative which reflects that the high aerodynamic damping of the flapping motion is the main source of the modal damping. E_{13} is positive which means that energy is transfered from body to flapping motion to cancel out the flap damping. This is also valid for all other modes. In fact, there exists a kind of energy balance between heavily damped flapping motion, lightly damped lead-lag motion and the body motion without damping. The modal damping is the result of this energy balance and in some extent determined by the ratio between these motions.

The influence of the ratio of helicopter inertia to rotor inertia is shown in Fig. 9.

The increase of instability with the decrease of $\bar{I}_h$ can be explained by the increase of inertial coupling due to the increase of blade mass.

For the nonisotropic case, minor opposite whirling motion is added to the original one-directional whirling motion and the basic characteristics of the isotropic case are still retained in this nonisotropic case. The diagram of mutual excitation is shown in Fig. 10.

The main source of instability is the positive mutual

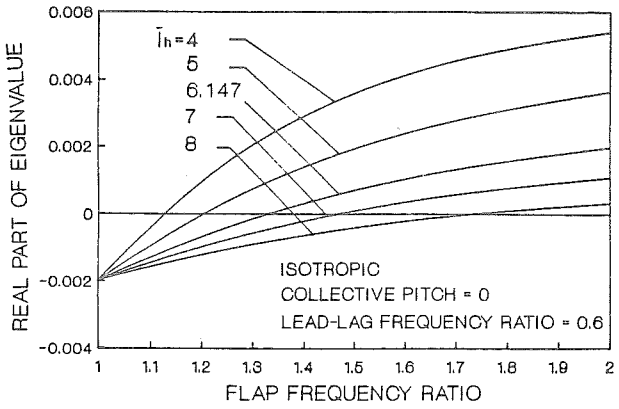

Fig. 9 The influence of $\bar{I}_h$ on instability of the LR mode (isotropic, $\bar{\omega}_\xi = 0.6, \theta = 0$)

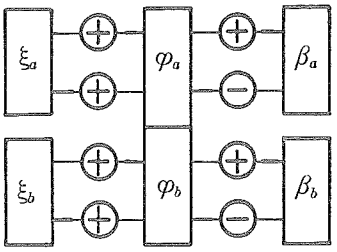

Fig. 10 Diagram of mutual excitation of the LR mode (nonisotropic, $\theta = 0$)

excitation between the forward whirling lead-lag motion ξ_a (regressive in the rotating coordinate) and the forward whirling body motion φ_a. The approximate expressions of E_{23a} and E_{32a} are still the same as Equation (13) except that I_2 should be changed into I_{2a}. The physical explanation and the influence of the main factors are still the same.

It is worthy of note that the instability increases with the increase of nonisotropy as shown in Fig. 11. This phenomenon can be explained by the reduction of helicopter roll inertia I_x in the nonisotropic case. Since the roll motion φ_x is predominant in this case, the reduction of I_x has the similar influence as the reduction of $\bar{I}_h$.

The Case with Collective Pitch

High collective pitch will induce high rotor lift and coning angle, and hence strong aerodynamic and inertial coupling between lead-lag motion and flapping motion. Ormiston[7] and King[8] pointed out the destabilizing effect of this flap-lag coupling which had been experimentally verified[8]. The mechanism of this destabilizing effect and its influence on the basic nature of the phenomenon is investigated as below.

The variation of eigenvalues with $\bar{\omega}_\beta$ at $\theta = 0.3$ is shown in Fig. 12. Modal damping of the LR and LA modes versus $\bar{\omega}_\xi$ at different collective pitch is shown in Fig. 13.

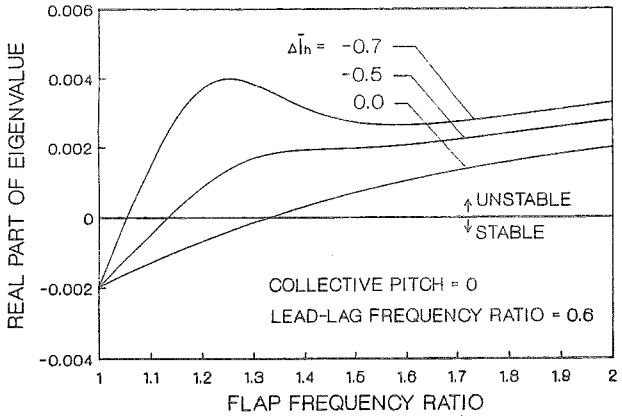

Fig. 11 The influence of $\delta\bar{I}_h$ on instability of the LR mode ($\bar{\omega}_\xi = 0.6, \theta = 0$)

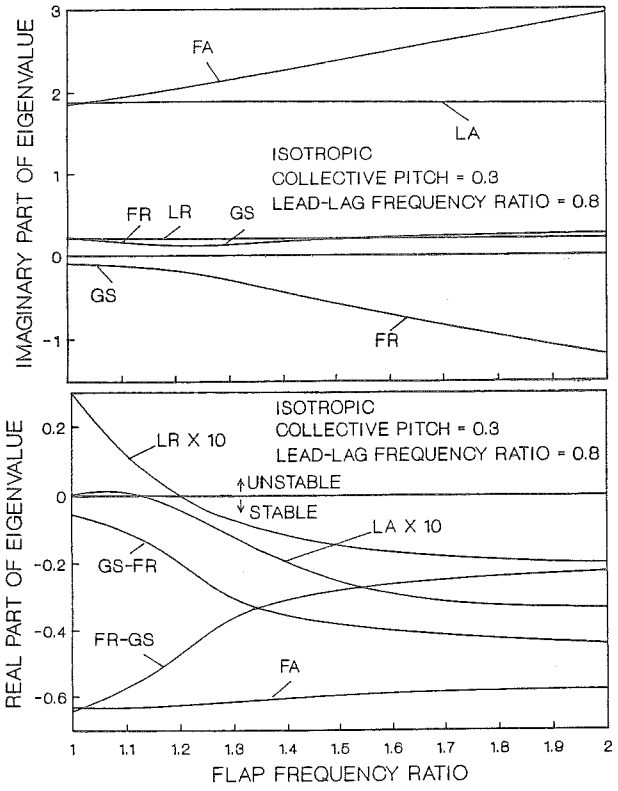

Fig. 12 Eigenvalue versus flap frequency ratio $\bar{\omega}_\beta$ (isotropic, $\bar{\omega}_\xi = 0.8, \theta = 0.3$)

Compared with the case of zero collective pitch, some significant distinctions can be observed. Not only the LR mode but also the LA mode can be unstable at high collective pitch and instability occurs within a certain $\bar{\omega}_\xi$ range and at low $\bar{\omega}_\beta$. The LR mode is unstable only in the soft-inplane region ($\bar{\omega}_\xi < 1$), but the unstable region of the LA mode extends from soft-inplane to stiff-inplane ($\bar{\omega}_\xi > 1$). The peak instability increases with collective pitch θ. The instability of the LR mode is much higher than that of the LA mode. The eigenvector

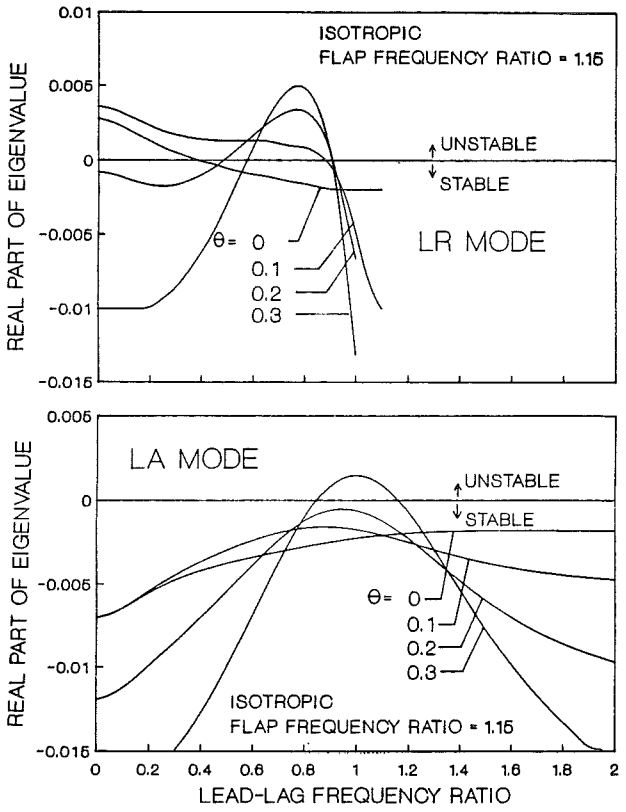

Fig. 13 Real part of eigenvalue versus $\bar{\omega}_\xi$ of the LR and LA modes (isotropic, $\bar{\omega}_\beta = 1.15$)

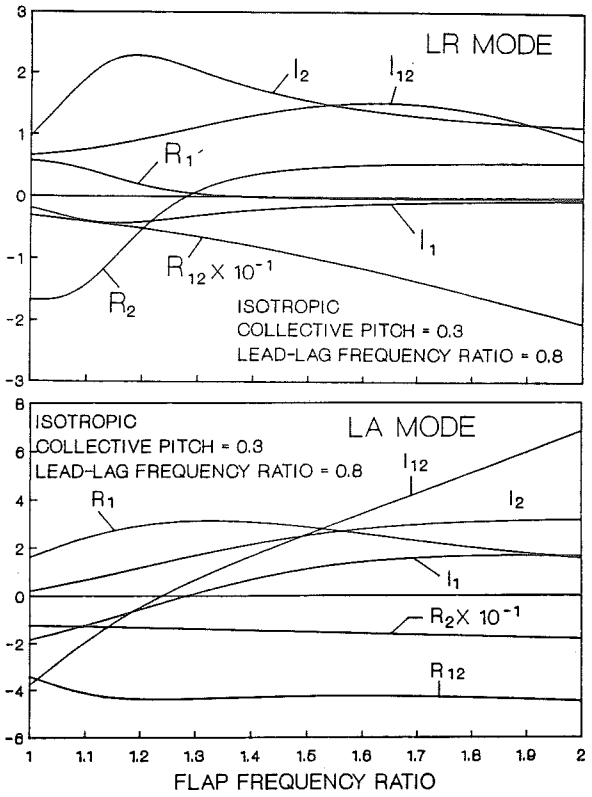

Fig. 14 Eigenvector of the LR and LA modes versus $\bar{\omega}_\beta$ (isotropic, $\bar{\omega}_\xi = 0.8, \theta = 0.3$)

and mutual excitation of the LR and LA modes are shown in Fig. 14 and 15. The diagram of mutual excitation in the unstable region is shown in Fig. 16.

For the LR mode there are two sources of instability: positive mutual excitation between ξ and β (E_{12}, E_{21}) and between ξ and φ (E_{23}, E_{32}). For the LA mode there is only one source of instability, the positive mutual excitation between ξ and β. The main part of E_{23} and E_{32} of the LR mode is still the inertial coupling expressed in equation (13). The approximate expressions of E_{12} and E_{21} (normalized to $|\beta|^2$) of both modes are

$$E_{12} = -(\gamma \frac{F}{2} - 2\beta_0)(\omega - 1)^2 R_{12}$$
$$E_{21} = -(2\beta_0 - \gamma \frac{t}{4})(\omega - 1)^2 R_{12} \qquad (14)$$

In the expression of E_{12} the term $\gamma \frac{F}{2}$ represents the aerodynamic flapping moment due to lead-lag velocity and the term $2\beta_0$ represents the inertial flapping moment due to lead-lag motion. $\gamma \frac{F}{2}$ is always greater than $2\beta_0$. In the expression of E_{21} the term $2\beta_0$ represents the inertial lead-lag moment due to flapping motion (Coriolis moment) and the term $\gamma \frac{t}{4}$ represents aerodynamic lead-lag moment due to flapping motion. Conventionally, $2\beta_0$ is greater than $\gamma \frac{t}{4}$. The expressions of β_0, F, and t are given in the Appendix. All of them increase with θ. In view of the negative value of R_{12}, both E_{12} and E_{21} are simultaneously positive. The physical explanation can be inferred from the relationship between flapping motion and lead-lag motion due to the negative R_{12} (Fig. 17).

The aerodynamic flapping moment due to lead-lag velocity is in phase with the blade flapping velocity, and the inertial lead-lag moment due to flapping velocity is also in phase with the blade lead-lag velocity.

In the case of isolated rotor system (fixed body) flap-lag instability can occur at high collective pitch. The source of instability is the above mentioned positive mutual excitation between ξ and β. Ormiston and Hodges pointed out that the center of unstable region is the frequency coalescence point of $\bar{\omega}_\beta$ and $\bar{\omega}_\xi$, and the instability increases with collective pitch θ.[9] For the rotor body coupled system, the instability of the LR mode at high collective pitch in fact is a combination of air resonance and flap-lag instability. There are significant influences of the ξ/φ inertial coupling on the phenomenon. The unstable region moves from the frequency coalescence point of the undamped $\bar{\omega}_\beta$ and $\bar{\omega}_\xi$ to a much lower $\bar{\omega}_\xi$ range limited to the soft-inplane region and the instability is agggravated due to the dual source of instability. The instability of the LA mode is still a kind of flap-lag instability influenced by the coupling with the body motion. The unstable region moves slightly to a lower $\bar{\omega}_\xi$ range and the instability is alleviated.

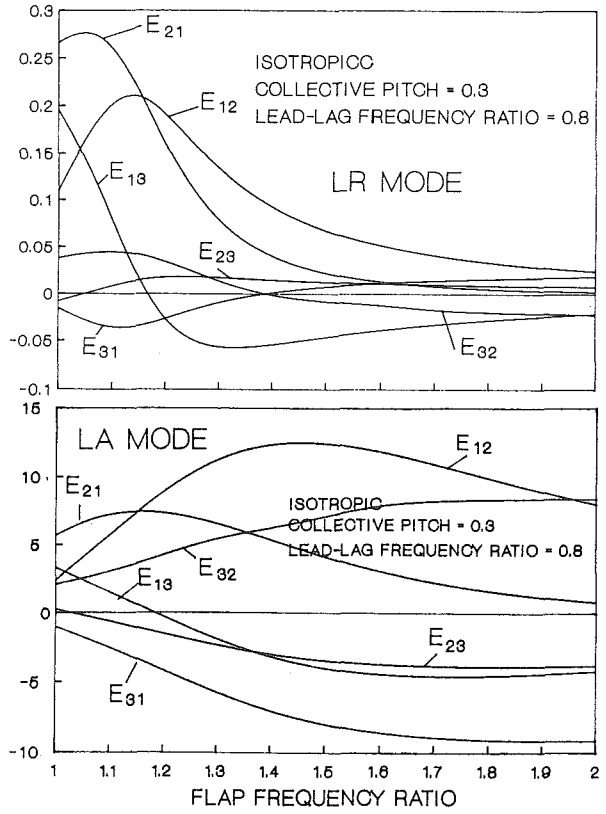

Fig. 15 Mutual excitation of the LR and LA modes (isotropic, $\bar{\omega}_\xi = 0.8, \theta = 0.3$)

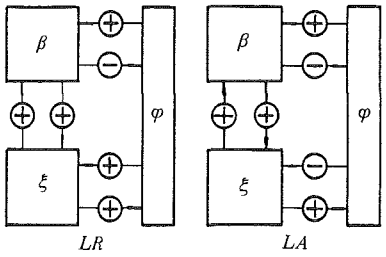

Fig. 16 Diagram of mutual excitation of the LR and LA modes in the unstable region (isotropic, $\theta = 0.3$)

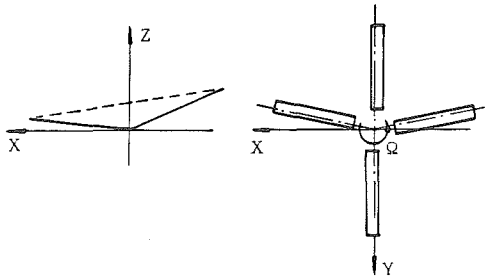

Fig. 17 Illustration of flapping motion and lead-lag motion due to negative R_{12}

For the nonisotropic case, the basic characteristics of the unstable LR and LA modes of the isotropic case are still retained.

The eigenvector and mutual excitation of these two modes in the unstable region are shown in Table 1.

Mode	$\bar{\omega}_\beta$	$\bar{\omega}_\xi$		$\sigma \times 10^2$	ω
LR	1.15	0.62		0.52	0.37
LA	1.15	0.97		0.08	2.08
R_{1a}	I_{1a}	R_{2a}	I_{2a}	R_{12a}	I_{12a}
0.43	− 0.87	− 3.04	4.46	− 5.52	− 0.76
2.08	− 1.80	− 9.09	0.60	− 2.65	− 2.00
R_{1b}	I_{1b}	R_{2b}	I_{2b}	R_{12b}	I_{12b}
− 0.44	− 0.43	− 0.18	0.10	0.09	− 0.33
− 0.16	− 1.06	− 0.44	0.02	0.05	− 0.41
R_3	I_3	E_{12a}	E_{21a}	E_{23a}	E_{32a}
0.63	0.20	0.54	0.55	0.15	0.63
0.52	0.001	6.13	6.12	− 1.09	13.48
E_{13a}	E_{31a}	E_{12b}	E_{21b}	E_{23b}	E_{32b}
− 0.06	− 0.10	− 0.007	− 0.007	0.077	− 0.016
4.95	− 2.84	− 0.037	− 0.035	3.51	− 0.21
E_{13b}	E_{31b}				
0.40	−0.023				
3.78	0.101				

Table 1 Eigenvalue, eigenvector and mutual excitation of the LR and LA modes in the unstable region (nonisotropic, $\delta\bar{I}_h = -0.5\bar{I}_h, \theta = 0.3$)

The diagram of mutual excitation in the unstable region is shown in Fig. 18.

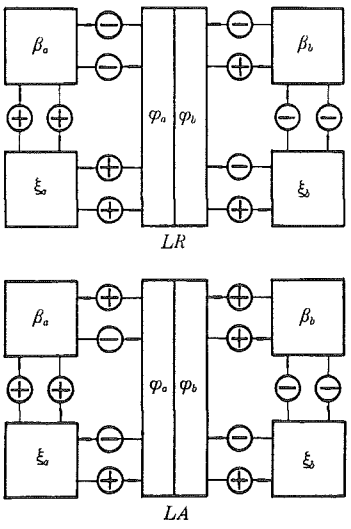

Fig. 18 Diagram of mutual excitation of the LR and LA modes (nonisotropic)

Although in the unstable region, minor backward whirling motions are added to the original forward whirling motions of the isotropic case, the mutual excitations between the forward whirling motions are still dominant. The analysis for the isotropic case is still valid for the nonisotropic case.

The Instability of Typical Rotor Types

Three typical rotor types are investigated.

Type 1: Hingeless rotor. The rotor blades are cantilevered. $\bar{\omega}_\beta$ and $\bar{\omega}_\xi$ decrease with rotor speed. At normal

rotor speed ($\Omega/\Omega_0=1$), $\bar{\omega}_\beta = 1.12, \bar{\omega}_\xi = 0.624$.

Type 2: Articulated rotor with elastical hinge restraint, such as the French Starflex rotor. Viscoelastic lag damper provides strong elastical restraint to the lag hinge. At normal rotor speed, $\bar{\omega}_\beta = 1.038, \bar{\omega}_\xi = 0.624$. The variation of $\bar{\omega}_\xi$ with rotor speed is the same as Type 1.

Type 3: Articulated rotor. At normal rotor speed, $\bar{\omega}_\beta = 1.038, \bar{\omega}_\xi = 0.25$, $\bar{\omega}_\beta$ and $\bar{\omega}_\xi$ are constant at different rotor speed.

The variation of $\bar{\omega}_\beta$ and $\bar{\omega}_\xi$ with rotor speed ratio for Type 1 and 2 is shown in Fig. 19.

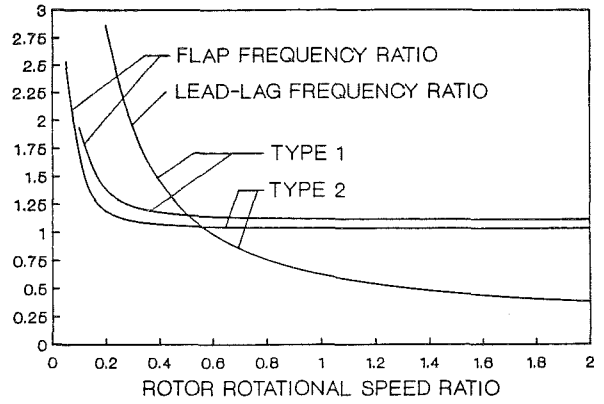

Fig. 19 Variation of $\bar{\omega}_\beta$ and $\bar{\omega}_\xi$ versus Ω/Ω_0

The variation of σ versus rotor speed ratio for the isotropic case is shown in Fig. 20 (Type 1) and Fig. 21 (Type 2). The modal damping is calculated at collective pitch $\theta = 0, 0.13, 0.3$. In the case of $\theta = 0.13$, the rotor lift at normal speed is approximately equal to helicopter weight. When $\theta = 0.3$, the rotor lift is approximately equal to three times helicopter weight. Of course, rotor lift is zero when $\theta = 0$. $\theta = 0$ and $\theta = 0.3$ can occur in maneuver.

Both type 1 and 2 can be unstable at normal speed range with normal or high collective pith ($\theta = 0.13$, 0.3), LR mode is more unstable than LA mode. Type 2 is more unstable than type 1. The reason is that $\bar{\omega}_\beta$ of type 2 is closer to $\bar{\omega}_\xi$ than type 1. Hence the mutual excitation between ξ and β is more serious. At zero collective pitch type 1 is less stable than type 2 which can be explained by the higher $\bar{\omega}_\beta$ of type 1. For the actual non-isotropic case, LR mode of type 1 can be unstable at high rotor speed.

For the articulated rotor (type 3), the LR mode is stable at zero collective pitch (Fig. 4) due to the low $\bar{\omega}_\beta$. The LR and LA modes are also stable at high collective pitch due to the low $\bar{\omega}_\xi$ (Fig. 13).

It is obvious from this analysis that the rotor with low flap frequency and high lead-lag frequency is more vulnerable to air resonance instability.

Conclusions

1. The source of instability for a multi-d. o. f. dynamic system is the mutual excitation between two or more d. o. f. and this is critical to the basic nature of the phenomenon.

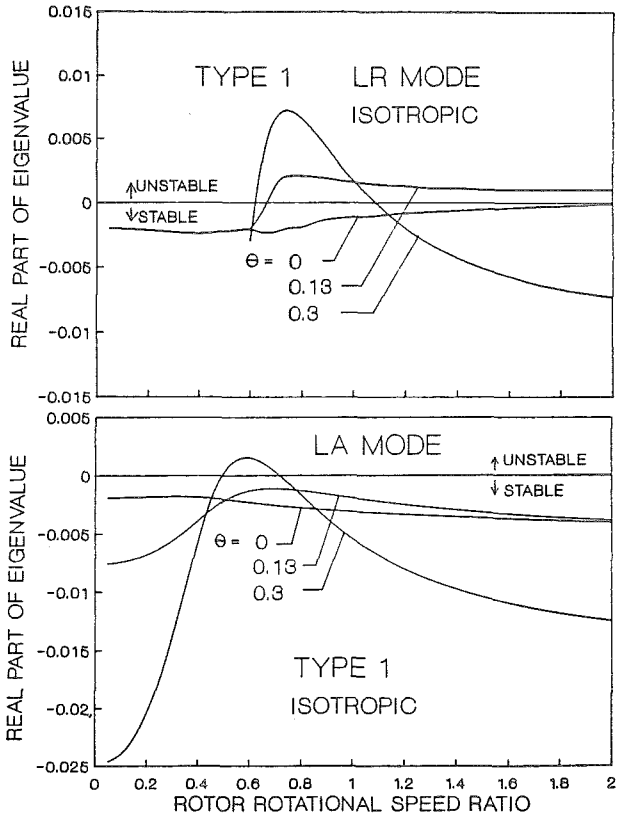

Fig. 20 Modal damping of the LR and LA modes (Type 1, isotropic)

2. The source of air resonance instability of the LR mode for the zero collective case is the mutual excitation between regressive lead-lag motion ξ and body forward whirling motion φ stemming from the inertial coupling of these two d. o. f..

3. For the case with high collective pitch, both LR and LA modes can be unstable. For the LA mode the only source of instability is the mutual excitaion between the lead-lag motion ξ and flap motion β originating from their inertial and aerodynamic coupling. There are two sources of instability for the LR mode: mutual excitation between ξ and φ and between ξ and β. The dual sources aggravate the instability.

4. The flap frequency $\bar{\omega}_\beta$ and lead-lag frequency $\bar{\omega}_\xi$ are the most important parameters which influence the instability. The rotor with high $\bar{\omega}_\beta$ and $\bar{\omega}_\xi$ (such as the hingeless rotor) and the rotor with low $\bar{\omega}_\beta$ and high $\bar{\omega}_\xi$ (such as the articulated rotor with lag hinge restraint) are more vulnerable to air resonance instability at normal or high collective pitch, especially the second type.

5. The other parameters are the ratio of helicopter inertia to rotor inertia $\bar{I}_h$ and the nonisotropy of helicopter inertia $\delta\bar{I}_h$. The instability increases with the decrease of $\bar{I}_h$ and the increase of nonisotropy.

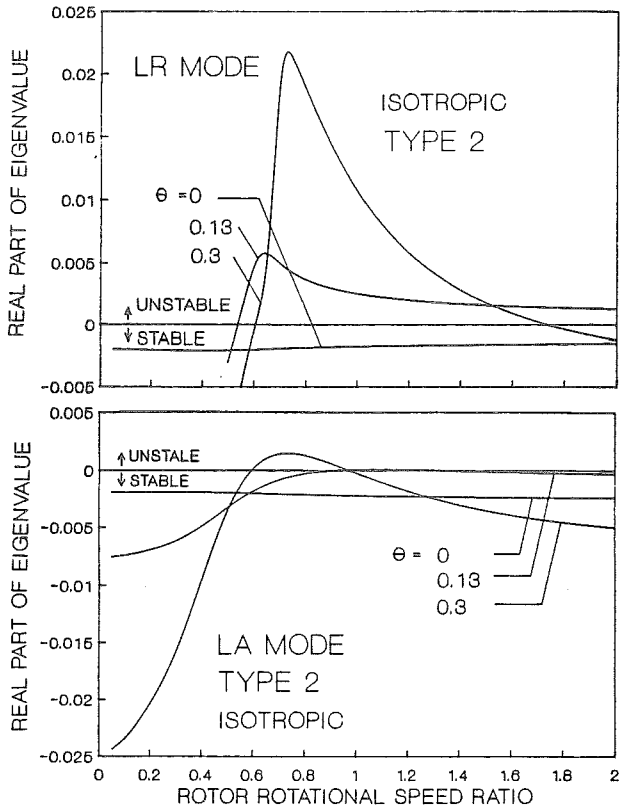

Fig. 21 Modal damping of the LR and LA modes (Type 2, isotropic)

Appendix

Each element of the M, C, and K matrices is a complex variable.

The elements of the isotropic case are given below

$$M_{11}=1 \qquad M_{12}=0 \qquad M_{13}=f_2 i$$
$$M_{21}=0 \qquad M_{22}=1 \qquad M_{23}=\frac{3}{2}h_2$$
$$M_{31}=-\frac{3}{2}\bar{h}\beta_0 i \qquad M_{32}=\frac{3}{2}\bar{h} \qquad M_{33}=\bar{I}_h+3\bar{h}\beta_0 \tag{A1}$$

$$C_{11}=\frac{\gamma}{4}-2i \qquad C_{12}=\frac{\gamma}{2}F-2\beta_0$$
$$C_{13}=2+\frac{2}{3}\gamma F h_1+\frac{\gamma}{4}f_1 i \qquad C_{21}=2\beta_0-\frac{\gamma}{4}t$$
$$C_{22}=\frac{\gamma}{2}C-2i \qquad C_{23}=\frac{2}{3}\gamma h_1 C-\frac{\gamma}{4}f_1 t i$$
$$C_{31}=-\frac{\gamma}{3}\bar{h}t-\frac{\gamma}{3}\bar{h}\beta_0 i \qquad C_{32}=\frac{2}{3}\gamma\bar{h}C-\frac{2}{3}\gamma\bar{h}F\beta_0 i$$
$$C_{33}=\gamma\bar{h}(h_2 C+\frac{1}{3}f_2\beta_0)-\gamma\bar{h}(\frac{1}{3}f_2 t+h_2 F\beta_0)i \tag{A2}$$

$$K_{11}=\bar{\omega}_\beta^2-1+\frac{\gamma}{2}F\beta_0-\frac{\gamma}{4}i$$
$$K_{12}=-(\frac{\gamma}{2}F-2\beta_0)i \qquad K_{13}=0$$
$$K_{21}=\frac{\gamma}{2}C\beta_0-(2\beta_0-\frac{\gamma}{4}t)i$$
$$K_{22}=\bar{\omega}_\xi^2-1-\frac{\gamma}{2}Ci \qquad K_{23}=0$$
$$K_{31}=\gamma(\frac{2}{3}\bar{h}C\beta_0-\frac{1}{3}\bar{h}\beta_0-\frac{D}{4})+[\bar{\omega}_\beta^2-1+\frac{\gamma}{3}\bar{h}(T+t-2\beta_0^2F)]i$$
$$K_{32}=(\bar{\omega}_\beta^2-1-\bar{\omega}_\xi^2-\frac{\gamma}{3}\bar{h}\theta)\beta_0-\gamma(\frac{1}{3}\bar{h}S-\frac{D}{4}\beta_0)i$$
$$K_{33}=0 \tag{A3}$$

$$A=\frac{a\sigma}{12}\left(\sqrt{1+\frac{24\theta}{a\sigma}}-1\right) \qquad C=\bar{C}_x+\frac{1}{2}\theta A$$
$$\bar{C}_x=\frac{C_x}{a} \qquad D=\bar{C}_x+A(\theta-A)$$
$$F=\theta-\frac{1}{2}A \qquad f_1=1+\frac{4}{3}\bar{h}\beta_0$$
$$f_2=1+\frac{3}{2}\bar{h}\beta_0 \qquad h_1=\bar{h}+\frac{3}{4}\beta_0$$
$$h_2=\bar{h}+\frac{2}{3}\beta_0 \qquad h_3=\bar{h}+\frac{1}{2}\beta_0$$
$$S=\bar{C}_x+A^2 \qquad T=\theta-A$$
$$t=\theta-2A \qquad \beta_0=\frac{\gamma}{4}\frac{T}{\bar{\omega}_\beta^2} \tag{A4}$$

References

1. Donham, R. E., Cardinale, S. V., and Sachs, I. B., "Ground and Air Resonance Characteristics of a Soft In-plane Rigid Rotor System," Journal of the American Helicopter Society, Vol. 14, (4), Oct. 1969.
2. Lytwyn, R. T., Miao, W., and Woitch, W., "Airborne and Ground Resonance of Hingeless Rotors", Journal of the American Helicopter Society, Vol. 16, (2) Apr. 1971.
3. Baldock, J. C. A., "Some Calculations for Air Resonance of a Helicopter with Non-Articulated Rotor Blades," A. R. C. R. & M. No. 3743, 1974.
4. Coleman, R. and Feignold, A. M., "Theory of Self-excited Mechanical Oscillations of Helicopter Rotors with Hinged Blades," NACA Report 1351, 1958.
5. Zhang, Xiaogu, "Physical Understanding of Helicopter Air and Ground Resonance", Journal of the American Helicopter Society, Vol. 31, (4), Oct. 1986.
6. Bielawa, R. L., "Notes Regarding Fundamental Understanding of Rotorcraft Aeroelastic Instability," Journal of the American Helicopter Society, Vol. 32, (4), Oct. 1987.
7. Ormiston, R. A., "Rotor-fuselage Dynamic Coupling Characteristics of Helicopter Air and Ground Resonance", The Theoretical Basis of Helicopter Technology Seminar, Nanjing, China, Nov. 1985.
8. King, S. P., "Theoretical and Experimental Investigations into Helicopter Air Resonance", Proceedings of the 39th Annual Forum of the American Helicopter Society, St. Louis, May 1983.
9. Ormiston, R. A. and Hodges, D. H., "Linear Flap-Lag Dynamics of Hingeless Helicopter Rotor Blades in Hover", Journal of the American Helicopter Sociely, Vol. 17, (2), April 1972.